RSC Advances

PAPER

View Article Online
View Journal | View Issue

Cite this: *RSC Adv.*, 2015, **5**, 85350

Synthesis of 1,3,5-trisubstituted pyrazoline derivatives and their applications†

Jugal V. Mehta,[a] Sanjay B. Gajera,[a] Parth Thakor,[b] Vasudev R. Thakkar[b] and Mohan N. Patel*[a]

A series of 1,3,5-trisubstituted pyrazolines based homoleptic Ru(III) complexes of type $[Ru(L^{1-7})_3]\cdot(PF_6)_3$ (L^{1-7} = pyrazoline ligands) have been synthesized and characterized by elemental analysis, electronic spectroscopy, conductance measurements, thermogravimetric analysis (TGA), electron paramagnetic resonance (EPR), fourier transform infrared (FT-IR) spectroscopy and liquid chromatography mass spectroscopy (LC-MS). Octahedral geometry around ruthenium has been assigned in all complexes using EPR and electronic spectral analysis. All complexes have been investigated for their interaction with Herring Sperm (HS) DNA utilizing an absorption titration (K_b = 2.42–6.07 × 10^5 M^{-1}) and viscosity measurement study. The studies suggest the classical intercalative mode of binding. The DNA-binding property of the Ru(III) complexes was also investigated theoretically using a molecular docking study and suggests an intercalation binding mode between the complex and nucleotide base pairs. A cleavage study on pUC19 DNA has been performed by agarose gel electrophoresis. The results indicated that the Ru(III) complexes can more effectively promote the cleavage of plasmid DNA. The free ligands and their complexes have been evaluated for cytotoxicity activity against *S. pombe* cells at a cellular level. A comparative study of cellular level cytotoxicity values of the all compounds indicates that the metal complexes show better activity against *S. pombe* cells compared to the pyrazoline ligands. The complexes have been screened for their *in vitro* antibacterial activity against two Gram(+ve) and three Gram(−ve) microorganisms. Ru(III) complexes are good *in vitro* cytotoxic agents and 50% lethal concentration (LC_{50}) values are in range of 5.296–7.925 μg mL^{-1}. All newly synthesized Ru(III) complexes have been also evaluated for their *in vitro* antimalarial activity against *Plasmodium falciparum* strain [inhibition concentration (IC_{50}) = 0.54–0.92 μg mL^{-1}].

Received 25th August 2015
Accepted 30th September 2015

DOI: 10.1039/c5ra17185g

www.rsc.org/advances

1. Introduction

The intercalation of transition metal complexes into DNA has been a topic of major bioinorganic interest in the past two decades and continues to receive much attention.[1,2] As a crucial target of anticancer drugs, DNA plays a central role in replication, transcription, and regulation of genes. The existence of metal-binding sites in the DNA structure makes different types of interaction possible. Small molecule binding to DNA can be reversible or irreversible, with the latter case usually involving covalent bond formation. Examples of irreversible binding agents include potent carcinogens such as aflatoxin B_1 and benzo[*a*]pyrene, and antitumour drugs such as cisplatin. Reversible recognition of nucleic acids characteristically involves non-covalent interactions and is usually defined by electrostatic, intercalative or major or minor groove binding motifs.[3] Within this context, this article centres on one particular area of research; transition metal complexes that function as reversible DNA binding agents.

Ruthenium complexes are enticing increasing attention as potential developed, particularly with ligands of biological relevance; the preferred octahedral coordination for the common +3 oxidation states in aqueous solution, together with adequate substitution rates and redox potentials for biological interactions and displayed low toxicity make ruthenium a particularly attractive choice for the development of new metallopharmaceuticals.[4,5]

Heterocyclic compounds have so far been synthesized mainly due to the wide range of biological activities. Much attention has been paid to the synthesis of heterocyclic compounds bearing nitrogen containing ring system, like pyrazoles mainly due to their higher pharmacological activity. Pyrazole and its derivatives are the key structural motifs in heterocyclic chemistry and occupy important position in medicinal chemistry. They exhibited a broad spectrum of pharmacological activities such as anticancer,[6] antibacterial,[7] antiviral,[8] analgesic,[9] anti-inflammatory,[10] antimalarial,

[a]*Sardar Patel University, Department of Chemistry, India. E-mail: jeneen@gmail.com*
[b]*Sardar Patel University, B. R. Doshi School of Biosciences, India*

† Electronic supplementary information (ESI) available. See DOI: 10.1039/c5ra17185g

antituberculosis and antifungal activities.[11] The inclusion of biologically-active ligands into metal complexes deals much scope for the design of novel drugs with improved and targeted activity. Studies on such complexes indicate that new mechanisms of action are favorable when combining the bioactivity of the ligand with the properties inherent to the metal, leading to the possibility of overcoming current drug resistance pathways.

In present study, a series of 1,3,5-trisubstituted pyrazolines based Ru(III) complexes have been synthesized and characterized by elemental analysis, electronic spectra, conductance measurements, TGA, EPR, FT-IR and LC-MS spectroscopy. All synthesized Ru(III) complexes were evaluated for their biological applications like DNA binding, DNA cleavage, antimalarial, antimicrobial and cellular level cytotoxicity. This study mainly focuses on exploring the trend in DNA-binding affinities of Ru(III) complexes and the important differences in some related properties. Understanding the features that contribute to recognition of DNA by small molecules or metal complexes is essential for the improvement of drugs targeted at DNA.

2. Materials and methods

2.1 Materials and reagents

All the chemicals and solvents were of reagent grade and used as purchased; double distilled water was used throughout the studies. $RuCl_3 \cdot 3H_2O$ was purchased from Chemport (Mumbai, India). *p*-Methylacetophenone, *p*-fluorobenzaldehyde, *p*-chlorobenzaldehyde, *p*-bromobenzaldehyde, *p*-methoxybenzaldehyde, *m*-chlorobenzaldehyde, *m*-bromobenzaldehyde, *p*-fluorobenzaldehyde, benzohydrazide, potassium *tert*-butoxide (PTB), KPF_6, HS DNA and EDTA were purchased from Sigma Aldrich Chemical Co. (India). Agarose, Luria Broth (LB), ethidium bromide (EtBr), Tris–acetyl–EDTA (TAE), bromophenol blue and xylene cyanol FF were purchased from Himedia (India). *S. pombe* Var. Paul Linder 3360 was obtained from IMTECH, Chandigarh.

2.2 Physical measurements

X-band electron paramagnetic resonance (EPR) spectra were recorded with a Varian E-line Century Series Spectrometer equipped with a dual cavity and operating at X-band (~9.5 GHz) with 100 kHz modulation frequency at room temperature. TCNE was used as field marker. The ^{1}H NMR and ^{13}C NMR were recorded with a Bruker Avance (400 MHz). IR spectra were recorded on a FT-IR Shimadzu spectrophotometer with sample prepared as KBr pellets in the range 4000–400 cm^{-1}. C, H, and N elemental analyses were performed with a model Perkin-Elmer 240 elemental analyser. Melting points (°C, uncorrected) were determined in open capillaries on hermoCal_{10} melting point apparatus (Analab Scientific Pvt. Ltd, India). Precoated silica gel plates (silica gel 0.25 mm, 60 G F 254; Merck, Germany) were used for thin layer chromatography. The LC-MS spectra were recorded using Thermo scientific mass spectrophotometer (USA). The electronic spectra were recorded on a UV-160A UV-vis spectrophotometer, Shimadzu, Kyoto (Japan). The magnetic moments were measured by Gouy's method using mercury tetrathiocyanatocobaltate(II) as the calibrant ($\chi_g = 16.44 \times 10^{-6}$ cgs units at 20 °C), citizen balance. Antibacterial study was carried out by means of laminar air flow cabinet Toshiba, Delhi (India). The thermogram of complexes was recorded with a Mettler Toledo TGA/DSC 1 thermogravimetric analyser. Conductance measurement was carried out using conductivity meter model number E-660A. Photo quantization of the gel after electrophoresis was done using AlphaDigiDoc™ RT. Version V.4.0.0 PC-Image software, California (USA).

2.3 Synthesis of the ligands

2.3.1 General method for synthesis of enones (chalcones) (3a–3g). To the solution of *p*-methyl acetophenone (**1**) (10 mmol, 1.34 mL) in 10 mL of methanol, freshly prepared methanolic KOH solution (20 mmol, 1.12 g, 25 mL) was added and stirred for 15 min. To this appropriate aldehyde (**2a–g**) (10 mmol) was added and the reaction mixture was stirred at room temperature for 24 h. The reaction mixture was cooled on an ice bath and neutralized with dilute hydrochloric acid. The precipitate appeared was separated by filtration and washed three times with 60 mL distilled water to give the crude product. The obtained product was recrystallized from methanol. The purity of the products was checked on TLC by using mixture of ethyl acetate and hexane as mobile phase.

2.3.2 General method for synthesis of 1,3,5-trisubstituted pyrazolines (5a–5g). To the solution of the appropriate enones (**3a–3g**) (6 mmol) in 10 mL of methanol, benzohydrazide (**4**) (6 mmol) and freshly prepared methanolic potassium *tert*-butoxide (PTB) (3 mmol, 0.34 g) solution were added and the reaction mixture was refluxed for 5–6 h. Conversion was monitored in every 60 min interval on precoated silica TLC plates by using mixture of ethyl acetate and hexane as mobile phase. The excess of solvent was removed under reduced pressure and the reaction mixture was cooled on an ice bath. The products precipitated out at low temperature were washed five times with 60 mL distilled water, reconstituted in minimum amount of methanol and dried under reduced pressure. The proposed reaction for the synthesis of ligands **5a–5g** is shown in Scheme 1. ^{1}H NMR, ^{13}C NMR, LC-mass and FT-IR spectra of ligands are shown in ESI material 1, 2, 3 and 4† respectively.

*2.3.2.1 [5-(4-Fluorophenyl)-3-(p-tolyl)-4,5-dihydro-1H-pyrazol-1-yl]-phenyl methanone (**5a**).* Prepared by above method from 3-(4-fluorophenyl)-1-(*p*-tolyl) prop-2-en-1-one (**3a**) (6 mmol, 1.44 g) and benzohydrazide (6 mmol, 0.82 g) after 5–6 h reflux; yield: 80%; white amorphous solid. mp: ≥ 200 °C; mol. wt. 358.41 g mol^{-1}; anal. calc. for: $C_{23}H_{19}FN_2O$, calc. (found) (%): C, 77.08 (77.01); H, 5.34 (5.20); N, 7.82 (7.73); ^{1}H NMR (400 MHz, $CDCl_3$-d_1) δ/ppm: 2.420 (3H, s, 4′-CH_3), 3.191 (1H, dd, $J = 5.2$ Hz, 17.6 Hz, 4-H_a), 3.791 (1H, dd, $J = 11.6$ Hz, 17.6 Hz, 4-H_b), 5.816 (1H, dd, $J = 5.2$ Hz, 12.0 Hz, 5-H), 7.523–7.029 (9H, m, 2″,3″,5″,6″,2‴,3‴,4‴,5‴,6‴-H), 7.637 (2H, d, $J = 8.4$ Hz, 2′-H & 6′-H), 8.065 (2H, d, $J = 7.2$ Hz, 3′-H & 5′-H); ^{13}C NMR (100 MHz, $CDCl_3$-d_1) δ/ppm: 167.67 (C═O), 160.97 ($C_{4''}$), 154.68 (C_3), 140.90 ($C_{4'}$), 137.76 ($C_{1''}$), 134.26 ($C_{1'''}$), 130.99 ($C_{4'''}$), 130.15 ($C_{3',5'}$), 129.48 ($C_{3''',5'''}$), 128.48 ($C_{1'}$), 127.58 ($C_{2'',6''}$), 127.50 ($C_{2''',6'''}$), 126.75 ($C_{2',6'}$), 115.92 ($C_{3'',5''}$), 60.66 (C_5), 41.51 (C_4), 21.53 (–CH_3); IR (KBr, 4000–400 cm^{-1}): 3071, ν(C–H)$_{ar\ stretching}$; 2931,

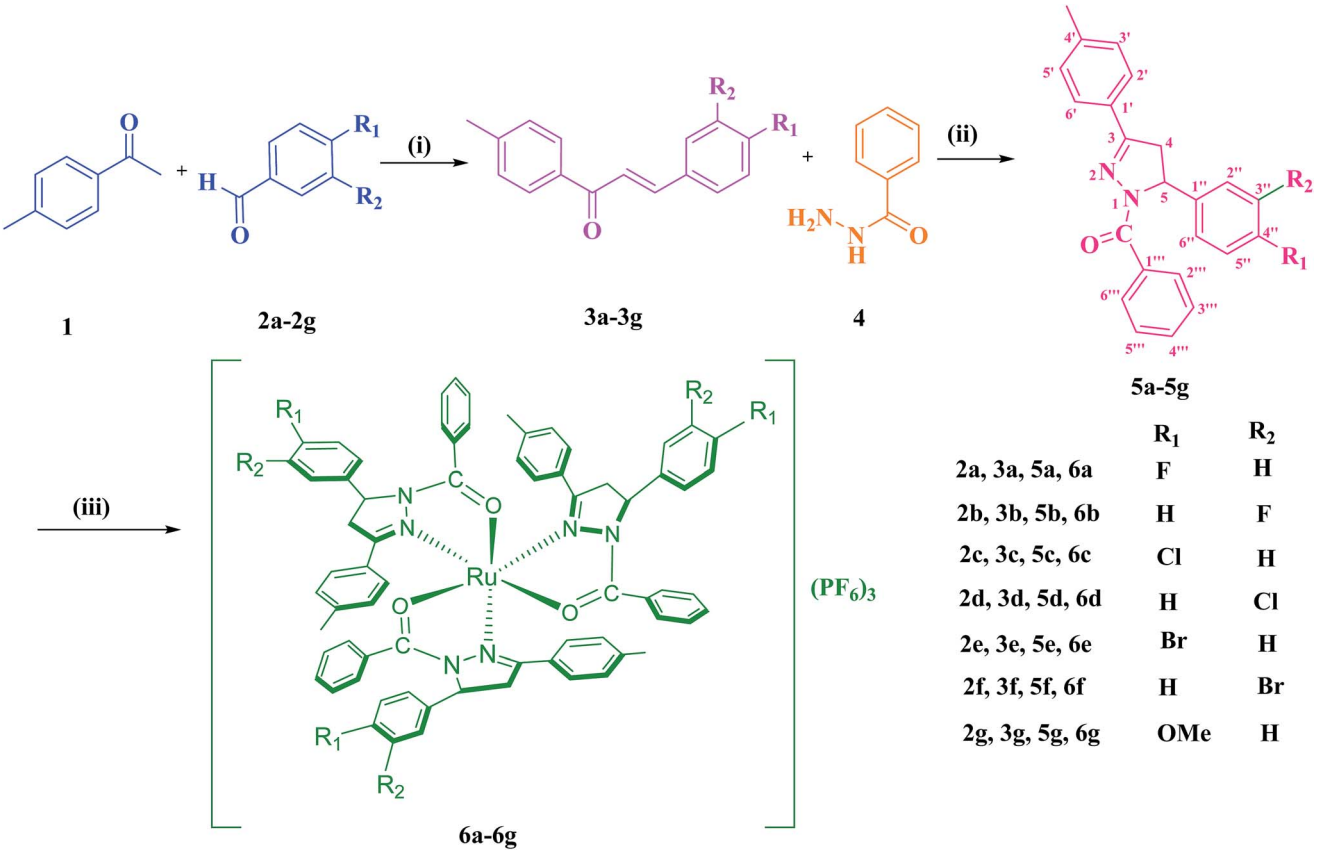

Reagents and conditions: (i) Methanolic KOH, r.t, 24 h; (ii) Methanol, potassium tert-butoxide, reflux 5-6 h; (iii) Methanol, $RuCl_3.3H_2O$, reflux 12 h, KPF_6

Scheme 1 Synthesis of 1,3,5-trisubstituted pyrazoline ligands (**5a–5g**) and its complexation with ruthenium metal ion.

ν(C–H)$_{al\ stretching}$; 1635, ν(C=O); 1508, ν(C=N); 1332, ν(C=C); 1220, ν(C–F); 1137, ν(C–N); 1095, 825, (*p*-substituted aromatic ring); 786, ν(C–H)$_{ar\ bending}$, LC-MS (*m*/*z*%): 359 (100) [M^+].

*2.3.2.2 [5-(3-Fluorophenyl)-3-(p-tolyl)-4,5-dihydro-1H-pyrazol-1-yl]-phenyl methanone (**5b**).* Prepared by above method from 3-(3-fluorophenyl)-1-(*p*-tolyl) prop-2-en-1-one (**3b**) (6 mmol, 1.44 g) and benzohydrazide (6 mmol, 0.82 g) after 5–6 h reflux; yield: 75%; white amorphous solid. mp: ≥ 200 °C; mol. wt. 358.41 g mol^{-1}; anal. calc. for: $C_{23}H_{19}FN_2O$, calc. (found) (%): C, 77.08 (77.02); H, 5.34 (5.26); N, 7.82 (7.75); ^{1}H NMR (400 MHz, $CDCl_3$-d_1) δ/ppm: 2.341 (3H, s, 4′-CH_3), 3.201 (1H, dd, J = 5.2 Hz, 18.4 Hz, 4-H_a), 3.907 (1H, dd, J = 12.0 Hz, 18.0 Hz, 4-H_b), 5.789 (1H, dd, J = 4.8 Hz, 11.6 Hz, 5-H), 7.551–7.096 (9H, m, 2″,4″,5″,6″,2‴,3‴,4‴,5‴,6‴-H), 7.616 (2H, d, J = 8.0 Hz, 2′-H & 6′-H), 7.898 (2H, d, J = 7.2 Hz, 3′-H & 5′-H); ^{13}C NMR (100 MHz, $CDCl_3$-d_1) δ/ppm: 167.92 (C=O), 161.95 ($C_{5''}$), 154.69 (C_3), 144.41 ($C_{1''}$), 140.94 ($C_{4'}$), 134.17 ($C_{1'''}$), 131.06 ($C_{4'''}$), 130.62 ($C_{3''',5'''}$), 130.18 ($C_{3''}$), 129.49 ($C_{3',5'}$), 128.40 ($C_{1'}$), 127.69 ($C_{2''',6'''}$), 126.77 ($C_{2',6'}$), 121.38 ($C_{2''}$), 114.78 ($C_{6''}$), 112.85 ($C_{4''}$), 60.73 (C_5), 41.44 (C_4), 21.54 (–CH_3); IR (KBr, 4000–400 cm^{-1}): 3050, ν(C–H)$_{ar\ stretching}$; 2934, ν(C–H)$_{al\ stretching}$; 1655, ν(C=O); 1496, ν(C=N); 1336, ν(C=C); 1249, ν(C–F); 1028, ν(C–N); 818, (*m*-substituted aromatic ring); 792, ν(C–H)$_{ar\ bending}$, LC-MS (*m*/*z*%): 359 (100) [M^+].

*2.3.2.3 [5-(4-Chlorophenyl)-3-(p-tolyl)-4,5-dihydro-1H-pyrazol-1-yl]-phenyl methanone (**5c**).* Prepared by above method from 3-(4-chlorophenyl)-1-(*p*-tolyl) prop-2-en-1-one (**3c**) (6 mmol, 1.54 g) and benzohydrazide (6 mmol, 0.82 g) after 5–6 h reflux; yield: 78%; white amorphous solid. mp: ≥ 200 °C; mol. wt. 374.86 g mol^{-1}; anal. calc. for: $C_{23}H_{19}ClN_2O$, calc. (found) (%): C, 73.69 (73.55); H, 5.11 (5.02); N, 7.47 (7.33); ^{1}H NMR (400 MHz, $CDCl_3$-d_1) δ/ppm: 2.414 (3H, s, 4′-CH_3), 3.179 (1H, dd, J = 5.2 Hz, 17.6 Hz, 4-H_a), 3.800 (1H, dd, J = 11.6 Hz, 17.6 Hz, 4-H_b), 5.798 (1H, dd, J = 4.8 Hz, 11.6 Hz, 5-H), 7.542–7.229 (9H, m, 2″,3″,5″,6″,2‴,3‴,4‴,5‴,6‴-H), 7.621 (2H, d, J = 8.4 Hz, 2′-H & 6′-H), 8.047 (2H, d, J = 7.2 Hz, 3′-H & 5′-H); ^{13}C NMR (100 MHz, $CDCl_3$-d_1) δ/ppm: 160.67 (C=O), 154.63 (C_3), 142.40 ($C_{4''}$), 140.93 ($C_{1''}$), 140.46 ($C_{4'}$), 133.47 ($C_{1'''}$), 131.02 ($C_{4'''}$), 130.15 ($C_{3',5'}$), 129.48 ($C_{3''',5'''}$), 129.12 ($C_{3'',5''}$), 128.43 ($C_{1'}$), 127.65 ($C_{2''',6'''}$), 127.24 ($C_{2'',6''}$), 126.75 ($C_{2',6'}$), 60.64 (C_5), 41.48 (C_4), 21.51 (–CH_3); IR (KBr, 4000–400 cm^{-1}): 3035, 3062, ν(C–H)$_{ar\ stretching}$; 2934, ν(C–H)$_{al\ stretching}$; 1635, ν(C=O); 1492, ν(C=N); 1336, ν(C=C); 1010, ν(C–N); 1177, ν(C–Cl); 1086, 821, (*p*-substituted aromatic ring); 789, ν(C–H)$_{ar\ bending}$, LC-MS (*m*/*z*%): 375 (100) [M^+], 377 [M + 2].

*2.3.2.4 [5-(3-Chlorophenyl)-3-(p-tolyl)-4,5-dihydro-1H-pyrazol-1-yl]-phenyl methanone (**5d**).* Prepared by above method from 3-(3-chlorophenyl)-1-(*p*-tolyl) prop-2-en-1-one (**3d**) (6 mmol, 1.54 g) and benzohydrazide (6 mmol, 0.82 g) after 5–6 h reflux; yield: 82%; white amorphous solid. mp: ≥ 200 °C; mol. wt. 374.86 g mol^{-1}; anal. calc. for: $C_{23}H_{19}ClN_2O$, calc. (found) (%): C, 73.69 (73.56); H, 5.11 (5.02); N, 7.47 (7.35); ^{1}H NMR (400 MHz, $CDCl_3$-d_1) δ/ppm: 2.415 (3H, s, 4′-CH_3), 3.190 (1H, dd, J = 5.2 Hz, 18.0 Hz, 4-H_a), 3.803 (1H, dd, J = 12.0 Hz, 17.6 Hz, 4-H_b), 5.79 (1H, dd, J = 5.2 Hz, 12.0 Hz, 5-H), 7.547–7.230 (9H, m, 2″,4″,5″,6″,2‴,3‴,4‴,5‴,6‴-H), 7.624 (2H, d, J = 8.0 Hz, 2′-H & 6′-H), 8.067 (2H, d, J = 7.2 Hz, 3′-H & 5′-H); ^{13}C NMR (100 MHz, $CDCl_3$-d_1) δ/ppm: 164.29 (C═O), 160.99 ($C_{5''}$), 154.69 (C_3), 143.92 ($C_{1''}$), 140.96 ($C_{4'}$), 134.82 ($C_{1'''}$), 131.07 ($C_{4'''}$), 130.27 ($C_{3''',5'''}$), 130.18 ($C_{3',5'}$), 129.48 ($C_{2''',6'''}$), 128.36 ($C_{1'}$), 127.94 ($C_{2',6'}$), 127.68 ($C_{3''}$), 126.77 ($C_{2''}$), 125.92 ($C_{6''}$), 123.99 ($C_{4''}$), 60.72 (C_5), 41.51 (C_4), 21.53 (–CH_3); IR (KBr, 4000–400 cm^{-1}): 3071, ν(C–H)$_{ar}$; 2931, ν(C–H)$_{al\ stretching}$; 1646, ν(C═O); 1492, ν(C═N); 1336, ν(C═C); 1073, ν(C–Cl); 1035, ν(C–N); 825, (*m*-substituted aromatic ring); 791, ν(C–H)$_{ar\ bending}$, LC-MS (*m*/*z*%): 375 (100) [M^+], 377 [M + 2].

*2.3.2.5 [5-(4-Bromophenyl)-3-(p-tolyl)-4,5-dihydro-1H-pyrazol-1-yl]-phenyl methanone (**5e**).* Prepared by above method from 3-(4-bromophenyl)-1-(*p*-tolyl) prop-2-en-1-one (**3e**) (6 mmol, 1.81 g) and benzohydrazide (6 mmol, 0.82 g) after 5–6 h reflux; yield: 76%; white amorphous solid. mp: ≥ 200 °C; mol. wt. 419.31 g mol^{-1}; anal. calc. for: $C_{23}H_{19}BrN_2O$, calc. (found) (%): C, 65.88 (65.78); H, 4.57 (4.48); N, 6.68 (6.55); ^{1}H NMR (400 MHz, $CDCl_3$-d_1) δ/ppm: 2.413 (3H, s, 4′-CH_3), 3.176 (1H, dd, J = 4.8 Hz, 17.6 Hz, 4-H_a), 3.798 (1H, dd, J = 11.6 Hz, 17.6 Hz, 4-H_b), 5.782 (1H, dd, J = 4.8 Hz, 11.6 Hz, 5-H), 7.542–7.229 (9H, m, 2″,3″,5″,6″,2‴,3‴,4‴,5‴,6‴-H), 7.619 (2H, d, J = 8.0 Hz, 2′-H & 6′-H), 8.045 (2H, d, J = 7.6 Hz, 3′-H & 5′-H); ^{13}C NMR (100 MHz, $CDCl_3$-d_1) δ/ppm: 160.16 (C═O), 154.66 (C_3), 140.97 ($C_{1'}$), 139.07 ($C_{1''}$), 137.96 ($C_{1'''}$), 132.07 ($C_{4'''}$), 131.05 ($C_{3''',5''}$), 130.16 ($C_{3''',5'''}$), 129.49 ($C_{3',5'}$), 128.39 ($C_{1'}$), 127.67 ($C_{2''',6'''}$), 127.57 ($C_{2'',6''}$), 126.76 ($C_{2',6'}$), 121.58 ($C_{4''}$), 60.70 (C_5), 41.43 (C_4), 21.54 (–CH_3); IR (KBr, 4000–400 cm^{-1}): 3057, ν(C–H)$_{ar\ stretching}$; 2950, ν(C–H)$_{al\ stretching}$; 1627, ν(C═O); 1492, ν(C═N); 1336, ν(C═C); 1029, ν(C–Br); 1010, ν(C–N); 1070, 818, (*p*-substituted aromatic ring); 778, ν(C–H)$_{ar\ bending}$, LC-MS (*m*/*z*%): 420.95 (100) [M^+], 422.80 [M + 2].

*2.3.2.6 [5-(3-Bromophenyl)-3-(p-tolyl)-4,5-dihydro-1H-pyrazol-1-yl]-phenyl methanone (**5f**).* Prepared by above method from 3-(3-bromophenyl)-1-(*p*-tolyl) prop-2-en-1-one (**3f**) (6 mmol, 1.81 g) and benzohydrazide (6 mmol, 0.82 g) after 5–6 h reflux; yield: 78%; white amorphous solid. mp: ≥ 200 °C; mol. wt. 419.31 g mol^{-1}; anal. calc. for: $C_{23}H_{19}BrN_2O$, calc. (found) (%): C, 65.88 (65.80); H, 4.57 (4.49); N, 6.68 (6.54); ^{1}H NMR (400 MHz, $CDCl_3$-d_1) δ/ppm: 2.345 (3H, s, 4′-CH_3), 3.219 (1H, dd, J = 5.2 Hz, 18.0 Hz, 4-H_a), 3.899 (1H, dd, J = 12.0 Hz, 18.4 Hz, 4-H_b), 5.769 (1H, dd, J = 5.2 Hz, 12.0 Hz, 5-H), 7.554–7.264 (9H, m, 2″,4″,5″,6″,2‴,3‴,4‴,5‴,6‴-H), 7.620 (2H, d, J = 8.0 Hz, 2′-H & 6′-H), 7.892 (2H, d, J = 7.2 Hz, 3′-H & 5′-H); ^{13}C NMR (100 MHz, $CDCl_3$-d_1) δ/ppm: 166.33 (C═O), 160.34 ($C_{5''}$), 154.64 (C_3), 144.19 ($C_{1''}$), 140.96 ($C_{4'}$), 134.12 ($C_{1'''}$), 131.07 ($C_{4'''}$), 130.88 ($C_{3''',5'''}$), 130.56 ($C_{3',5'}$), 130.19 ($C_{2''',6'''}$), 129.71 ($C_{2',6'}$), 128.84 ($C_{3''}$), 128.37 ($C_{1'}$), 127.69 ($C_{2''}$), 126.78 ($C_{6''}$), 124.46 ($C_{4''}$), 60.69 (C_5), 41.53 (C_4), 21.53 (–CH_3); IR (KBr, 4000–400 cm^{-1}): 3064, ν(C–H)$_{ar\ stretching}$; 2948, ν(C–H)$_{al\ stretching}$; 1633, ν(C═O); 1561, ν(C═N); 1336, ν(C═C); 1071, ν(C–Br); 1035, ν(C–N); 825, (*m*-substituted aromatic ring); 789, ν(C–H)$_{ar\ bending}$. LC-MS (*m*/*z*%): 419.05 (100) [M^+], 421.20 [M + 2].

*2.3.2.7 [5-(4-Methoxyphenyl)-3-(p-tolyl)-4,5-dihydro-1H-pyrazol-1-yl]-phenyl methanone (**5g**).* Prepared by above method from 3-(4-methoxyphenyl)-1-(*p*-tolyl) prop-2-en-1-one (**3g**) (6 mmol, 1.51 g) and benzohydrazide (6 mmol, 0.82 gm) after 5–6 h reflux; yield: 79%; white amorphous solid. mp: ≥ 200 °C; mol. wt. 370.44 g mol^{-1}; anal. calc. for: $C_{24}H_{22}N_2O_2$, calc. (found) (%): C, 77.81 (77.75); H, 5.99 (5.80); N, 7.56 (7.45); ^{1}H NMR (400 MHz, $CDCl_3$-d_1) δ/ppm: 2.414 (3H, s, 4′-CH_3), 3.212 (1H, dd, J = 4.8 Hz, 17.6 Hz, 4-H_a), 3.774 (1H, dd, J = 12.0 Hz, 17.6 Hz, 4-H_b), 3.799 (3H, s, 4″-OCH_3), 5.792 (1H, dd, J = 4.8 Hz, 11.6 Hz, 5-H), 7.524–6.878 (9H, m, 2″,3″,5″,6″,2‴,3‴,4‴,5‴,6‴-H), 7.632 (2H, d, J = 8.4 Hz, 2′-H & 6′-H), 8.045 (2H, d, J = 6.8 Hz, 3′-H & 5′-H); ^{13}C NMR (100 MHz, $CDCl_3$-d_1) δ/ppm: 166.25 (C═O), 159.06 ($C_{4''}$), 154.76 (C_3), 140.72 ($C_{4'}$), 134.53 ($C_{1'''}$), 134.19 ($C_{1''}$), 130.82 ($C_{4'''}$), 130.16 ($C_{3',5'}$), 129.43 ($C_{3''',5'''}$), 128.69 ($C_{1'}$), 127.59 ($C_{2''',6'''}$), 127.09 ($C_{2',6'}$), 126.75 ($C_{2'',6''}$), 114.30 ($C_{3'',5''}$), 60.68 (C_5), 55.30 (–OCH_3), 41.58 (C_4), 21.52 (–CH_3); IR (KBr, 4000–400 cm^{-1}): 3042, ν(C–H)$_{ar\ stretching}$; 2955 ν(C–H)$_{al\ stretching}$; 1691 ν(C═O); 1510 ν(C═N); 1332 ν(C═C); 1108 ν(C–N); 1256 ν(C–O–C)$_{sy}$; 1024 ν(C–O–C)$_{asy}$; 1075, 825 (*p*-substituted aromatic ring); 709 ν(C–H)$_{ar\ bending}$, LC-MS (*m*/*z*%): 371 (100) [M^+].

2.3.3 General synthesis of the complexes. The homoleptic Ru(III) metal complexes (**6a–6g**) of the general formula $[Ru(L)_3](PF_6)_3$ was synthesized by the reactions of $RuCl_3 \cdot 3H_2O$ with the respective ligands (**5a–5g**) in a 1 : 3 molar ratio in methanol.

*2.3.3.1 $[Ru^{III}$**(5a)**$_3](PF_6)_3$ **(6a).*** A methanolic suspension of the precursor $RuCl_3 \cdot 3H_2O$ (0.130 g, 0.5 mmol) was refluxed for 10 min. Then a solution of ligand **5a** (0.538 g, 0.15 mmol in 50 mL methanol), was added and the reaction was refluxed overnight yielding a red-brown solution. The reaction was filtered to remove the residual undissolved material. Then, a saturated solution of excess KPF_6 was added drop wise to the reaction mixture to complete precipitation and the mixture was kept at 4 °C overnight. The brown precipitate was filtered off, washed with water as well as diethyl ether and dried *in vacuo* at 35 °C. The proposed reaction for the synthesis of complexes **6a–6g** is shown in Scheme 1. Yield: 75.8%; mp: ≥ 300 °C; μ_{eff}: 1.86 BM; mol. wt. 1611.19 g mol^{-1}; anal. calc. for $C_{69}H_{57}F_{21}N_6O_3P_3Ru$, calc. (found) (%): C, 51.44 (51.22); H, 3.57 (3.40); N, 5.22 (5.15); Ru, 6.27 (6.20); IR (KBr, 4000–400 cm^{-1}): 3073, ν(C–H)$_{ar\ stretching}$; 2927, ν(C–H)$_{al\ stretching}$; 1604, ν(C═O); 1503, ν(C═N); 1340, ν(C═C); 1229, ν(C–F); 1162, ν(C–N); 1100, (*p*-substituted aromatic ring); 702, ν(C–H)$_{ar\ bending}$; 843, ν(PF_6); 560, ν(Ru–N); conductance: 175 Ω^{-1} cm^2 mol^{-1}; UV-vis: λ (nm) (ε, M^{-1} cm^{-1}): 575 (540), 308 (15 723), 237 (22 330).

*2.3.3.2 $[Ru^{III}$**(5b)**$_3](PF_6)_3$ **(6b).*** It was synthesized using ligand **5b** (0.538 g, 0.15 mmol). Yield: 74.0%; mp: ≥ 300 °C; μ_{eff}: 1.88 BM; mol. wt. 1611.19 g mol^{-1}; anal. calc. for $C_{69}H_{57}F_{21}N_6O_3P_3Ru$, calc. (found) (%): C, 51.44 (51.20); H, 3.57 (3.41); N, 5.22 (5.17); Ru, 6.27 (6.21); IR (KBr, 4000–400 cm^{-1}): 3072, ν(C–H)$_{ar\ stretching}$; 2927, ν(C–H)$_{al\ stretching}$; 1630, ν(C═O); 1489,

ν(C=N); 1343, ν(C=C); 1264, ν(C–F); 1042, ν(C–N); 810, (*m*-substituted aromatic ring); 789, $\nu(C–H)_{ar\ bending}$; 843, $\nu(PF_6)$; 557, ν(Ru–N); conductance: 180 Ω^{-1} cm^2 mol^{-1}; UV-vis: λ (nm) (ε, M^{-1} cm^{-1}): 593 (530), 315 (16 343), 260 (21 828).

2.3.3.3 $[Ru^{III}(5c)_3](PF_6)_3$ (6c). It was synthesized using ligand **5c** (0.562 g, 0.15 mmol). Yield: 72.0%; mp: ≥ 300 °C; μ_{eff}: 1.89 BM; mol. wt. 1660.55 g mol^{-1}; anal. calc. for $C_{69}H_{57}F_{18}Cl_3N_6O_3P_3Ru$, calc. (found) (%): C, 49.91 (49.35); H, 3.46 (3.40); N, 5.06 (5.01); Ru, 6.09 (6.02); IR (KBr, 4000–400 cm^{-1}): 3057, 3028, $\nu(C–H)_{ar\ stretching}$; 2925, $\nu(C–H)_{al\ stretching}$; 1626, ν(C=O); 1493, ν(C=N); 1333, ν(C=C); 1186, ν(C–Cl); 1014, ν(C–N); 1090, (*p*-substituted aromatic ring); 704, $\nu(C–H)_{ar\ bending}$; 848, $\nu(PF_6)$; 557, ν(Ru–N); conductance: 170 Ω^{-1} cm^2 mol^{-1}; UV-vis: λ (nm) (ε, M^{-1} cm^{-1}): 573 (565), 312 (16 760), 254 (25 720).

2.3.3.4 $[Ru^{III}(5d)_3](PF_6)_3$ (6d). It was synthesized using ligand **5d** (0.562 g, 0.15 mmol). Yield: 73.8%; mp: ≥ 300 °C; μ_{eff}: 1.92 BM; mol. wt. 1660.55 g mol^{-1}; anal. calc. for $C_{69}H_{57}F_{18}Cl_3N_6O_3P_3Ru$, calc. (found) (%): C, 49.91 (49.34); H, 3.46 (3.37); N, 5.06 (5.00); Ru, 6.09 (6.01); IR (KBr, 4000–400 cm^{-1}): 3065, $\nu(C–H)_{ar\ stretching}$; 2920, $\nu(C–H)_{al\ stretching}$; 1604, ν(C=O); 1453, ν(C=N); 1333, ν(C=C); 1079, ν(C–Cl); 1025, ν(C–N); 814, (*m*-substituted aromatic ring); 785, $\nu(C–H)_{ar\ bending}$; 843, $\nu(PF_6)$; 560, ν(Ru–N); conductance: 176 Ω^{-1} cm^2 mol^{-1}; UV-vis: λ (nm) (ε, M^{-1} cm^{-1}): 585 (535), 315 (17 322), 263 (24 825).

2.3.3.5 $[Ru^{III}(5e)_3](PF_6)_3$ (6e). It was synthesized using ligand **5e** (0.629 g, 0.15 mmol). Yield: 74.2%; mp: ≥ 300 °C; μ_{eff}: 1.90 BM; mol. wt. 1793.90 g mol^{-1}; anal. calc. for $C_{69}H_{57}F_{18}Br_3N_6O_3P_3Ru$, calc. (found) (%): C, 46.20 (46.12); H, 3.20 (3.13); N, 4.68 (4.59); Ru, 5.63 (5.55); IR (KBr, 4000–400 cm^{-1}): 3065, $\nu(C–H)_{ar\ stretching}$; 2927, $\nu(C–H)_{al\ stretching}$; 1594, ν(C=O); 1503, ν(C=N); 1340, ν(C=C); 1024, ν(C–Br); 999, ν(C–N); 1072, 782 (*p*-substituted aromatic ring); 782, $\nu(C–H)_{ar\ bending}$; 843, $\nu(PF_6)$; 557, ν(Ru–N); conductance: 174 Ω^{-1} cm^2 mol^{-1}; UV-vis: λ (nm) (ε, M^{-1} cm^{-1}): 570 (533), 325 (17 820), 245 (23 875).

2.3.3.6 $[Ru^{III}(5f)_3](PF_6)_3$ (6f). It was synthesized using ligand **5f** (0.629 g, 0.15 mmol). Yield: 76.8%; mp: ≥ 300 °C; μ_{eff}: 1.90 BM; mol. wt. 1793.90 g mol^{-1}; anal. calc. for $C_{69}H_{57}F_{18}Br_3N_6O_3P_3Ru$, calc. (found) (%): C, 46.20 (46.13); H, 3.20 (3.10); N, 4.68 (4.57); Ru, 5.63 (5.57); IR (KBr, 4000–400 cm^{-1}): 3036, $\nu(C–H)_{ar\ stretching}$; 2920, $\nu(C–H)_{al\ stretching}$; 1605, ν(C=O); 1540, ν(C=N); 1340, ν(C=C); 1075, ν(C–Br); 1010, ν(C–N); 782, (*m*-substituted aromatic ring); 756, $\nu(C–H)_{ar\ bending}$; 825, $\nu(PF_6)$; 560, ν(Ru–N); conductance: 195 Ω^{-1} cm^2 mol^{-1}; UV-vis: λ (nm) (ε, M^{-1} cm^{-1}): 587 (568), 320 (16 870), 253 (24 883).

2.3.3.7 $[Ru^{III}(5g)_3](PF_6)_3$ (6g). It was synthesized using ligand **5g** (0.556 g, 0.15 mmol). Yield: 73.5%; mp: ≥ 300 °C; μ_{eff}: 1.86 BM; mol. wt. 1647.29 g mol^{-1}; anal. calc. for $C_{72}H_{66}F_{18}N_6O_6P_3Ru$, calc. (found) (%): C, 52.50 (52.40); H, 4.04 (4.01); N, 5.10 (5.07); Ru, 6.14 (6.09); IR (KBr, 4000–400 cm^{-1}): 3043, $\nu(C–H)_{ar\ stretching}$; 2949, $\nu(C–H)_{al\ stretching}$; 1612, ν(C=O); 1514, ν(C=N); 1344, ν(C=C); 1253, $\nu(C–O–O)_{sy}$; 1032, $\nu(C–O–O)_{asy}$; 1104, ν(C–N); 1060, 810, (*p*-substituted aromatic ring); 702, $\nu(C–H)_{ar\ bending}$; 843, $\nu(PF_6)$; 560, ν(Ru–N); conductance: 192 Ω^{-1} cm^2 mol^{-1}; UV-vis: λ (nm) (ε, M^{-1} cm^{-1}): 595 (545), 318 (17 553), 256 (26 835).

2.4 Biological screening of synthesized complexes

2.4.1 *In vitro* antibacterial screening. The *in vitro* antibacterial activities of free ligands and ruthenium(III) complexes were tested against two Gram(+ve); *Staphylococcus aureus*, *Bacillus subtilis* and three Gram(−ve); *Serratia marcescens*, *Escherichia coli*, *Pseudomonas aeruginosa*, microorganisms. The MIC value was determined by broth dilution technique.[12] The detail experimental process is reported in newly published literatures.[13,14]

2.4.2 DNA binding study by absorption spectral analysis. DNA-mediated hypochromic and bathochromic shifts under the influence of the ruthenium complexes were measured with the help of UV-visible absorbance spectra. UV-visible spectral titration of Ru(III) complexes (in DMSO) with HS-DNA in phosphate buffer was carried out to inspect the binding mode for the complexes. The concentration of HS DNA was determined by measuring absorbance at 260 nm and using 12 858 M^{-1} cm^{-1} as the molar extinction coefficient value.[15] In experiment, fixed amount of DNA solution (100 μL) in phosphate buffer was added to sample cell holding in definite concentration of complex solution (20 μM) and reference cell to nullify the effect of HS DNA, and allowed to incubate for 10 min prior to the spectra being recorded. DMSO was also added into the reference cell as a control to nullify the effect of DMSO. The intrinsic binding constant, K_b, was determined by equation reported in published literatures.[13,14]

2.4.3 DNA binding study by hydrodynamic volume measurement. An Ubbelohde viscometer maintained at a constant temperature of 27 ± 0.1 °C in a thermostatic jacket, was used to measure the flow time of DNA in phosphate buffer (Na_2HPO_4/NaH_2PO_4, pH 7.2) with accuracy of 0.01 second and precision of 0.1 second. DNA samples, approximately 200 base pairs in average length, were prepared by sonicating in order to minimize complexities arising from DNA flexibility. Flow time for buffer alone was measured and was termed as t_0. The detail experimental process is reported in published literatures.[13,14]

2.4.4 Molecular docking study with HS DNA. The rigid molecular docking study has been performed using HEX 8.0 software to determine the orientation of the Ru(III) complexes binding to DNA. Docking was performed and the most stable configuration was chosen as input for investigation. The coordinates of metal complexes were taken from their optimized structure as a mol file and were converted to pdb format using CHIMERA 1.5.1 software. HS-DNA used in the experimental work was too large for current computational resources to dock, therefore, the structure of the DNA of sequence $d(ACCGACGTCGGT)_2$ (PDB id: 423D, a familiar sequence used in oligodeoxynucleotide study) obtained from the Protein Data Bank (http://www.rcsb.org/pdb). All calculations were carried out on an Intel CORE i3, 2.5 GHz based machine running MS Windows 8 64 bit as the operating system. The by default parameters were used for the docking calculation with correlation type shape only, FFT mode at 3D level, grid dimension of 6 with receptor range 180 and ligand range 180 with twist range 360 and distance range 40.[16]

2.4.5 DNA cleavage screening by chemical nuclease activity. Gel electrophoresis of pUC19 DNA was carried out in TAE buffer (0.04 M Tris–acetate, pH 8, 0.001 M EDTA). 15 μL reaction mixture containing 300 μg mL^{-1} plasmid DNA in TE buffer (10 mM Tris, 1 mM EDTA, pH 8.0) and 200 μM complex solution. Reactions were allowed to proceed for 3 h at 37 °C in dark and reactions were satiated by addition of 5 μL loading buffer (0.25% bromophenol blue, 40% sucrose, 0.25% xylene cyanol and 200 mM EDTA). The aliquots were loaded directly on to 1% agarose gel and electrophoresed at 50 V in 1 × TAE buffer. Gel was stained with 0.5 μg mL^{-1} ethidium bromide and was photographed on a UV illuminator. The percentage of each form of DNA was capacities. After electrophoresis, the proportion of DNA in each fraction was estimated quantitatively from the intensity of the bands using AlphaDigiDoc™ RT. Version V.4.0.0 PC-Image software. The degree of DNA cleavage activity was expressed in terms of the percentage of conversion of the SC-DNA to OC-DNA and L-DNA according equation reported in published literatures.[13,14,17]

2.4.6 *In vitro* cytotoxic study. Brine shrimp (Artemia cysts) eggs were hatched in a shallow rectangular plastic dish (22 × 32 cm), filled with artificial seawater, which was prepared with commercial salt mixture and double distilled water. An unequal partition was made in the plastic dish with the help of a perforated device. Approximately 50 mg of eggs were sprinkled into the large compartment and was opened to ordinary light. After two days, nauplii were collected by a pipette from the lighted side. A sample of the test compound was prepared by dissolving 10 mg of each compound in 10 mL of DMSO. From these stock solutions, solutions were transfer to 18 vials to make final concentration 2, 4, 8, 12, 16, and 20 mg mL^{-1} (three sets for each dilutions were used for each test sample and mean of three sets was used for LC_{50} calculation), and three vials were kept as control having same amount of DMSO only. When the nauplii were ready, 1 mL of seawater and 10 shrimps were added to each vial, and the volume was adjusted with seawater to 2.5 mL per vial. After 24 h, the number of survivors was counted.[18] Data were analyzed by simple logit method to determine the LC_{50} values, in which log of concentration of samples were plotted against percentage of mortality of nauplii.[19]

2.4.7 Cellular level bioassay. Cellular level bioassay was done using *S. pombe* cells, which were grown in liquid yeast extract media in 150 mL Erlenmeyer flask containing 50 mL of yeast extract media. Flask was incubated at 30 °C on shaker at 150 rpm till the exponential growth of *S. pombe* obtained (24 to 30 h). Then the cell culture was treated with the different concentrations (2, 4, 6, 8, 10 μg mL^{-1}) of synthesized complexes, free ligands and also with dimethyl sulphoxide (DMSO) as a control and further allowed to grow for 16–18 h. Next day, by centrifugation at 10 000 rpm 10 min; treated cells were collected and dissolved in 500 μL of PBS. The 80 μL of yeast culture dissolved in PBS and 20 μL of 0.4% trypan blue prepared in PBS were mixed and cells were observed in a compound microscope (40×). The dye could enter the dead cell only so they appeared blue whereas live cells resisted the entry of dye. The number of dead cells and number of live cells were counted in one field. Cell counting was repeated in two more of the microscopic fields and average percentage of cells died due to synthesized compounds were calculated.

2.4.8 *In vitro* antimalarial study. All the synthesized complexes were screened for their antimalarial activity against the *Plasmodium falciparum* strain. The *P. falciparum* strain was acquired from Shree R. B Shah Mahavir Super speciality hospital, Surat, Gujarat, India, and was used in *in vitro* tests. The *P. falciparum* strains were cultivated by a modified method described by Trager and Jensen.[20] The detail experimental process is reported in published literatures.[13,14]

3. Results and discussion

3.1 Magnetic moments, electronic spectra and conductance measurements

Magnetic moments measurement were carried out at room temperature for all the homoleptic Ru(III) complexes. The μ_{eff} values were obtained in the range of 1.78–1.93 BM, which corresponds to a single unpaired electron in low-spin $4d^5$ configuration and confirms the +3 oxidation state of ruthenium in the all complexes. The μ_{eff} values suggest a low-spin t_{2g}^5 configuration for ruthenium(III) ion in an octahedral environment.[21]

The electronic spectra of all the complexes in DMSO showed three bands in the region 237–595 nm. The ground state of Ru(III) (t_{2g}^5 configuration) is $^2T_{2g}$.[22] In most of the Ru(III) complexes, the electronic spectra show only charge transfer bands.[23] In $4d^5$ system, especially in Ru(III), which has relatively high oxidation properties, the charge transfer bands of the type $L_y \rightarrow t_{2g}$ are prominent in the low energy region and obscure the weaker bands due to d–d transition at 570–595 nm (ε = 533−745 M^{-1} cm^{-1}). The spectral profiles in UV region (below 400 nm) are very similar and are ligand centered transitions. These bands have been designated as π–π* [308–325 nm (ε = 15 723–17 820 M^{-1} cm^{-1})] and n–π* [237–263 nm (ε = 22 330–24 825 M^{-1} cm^{-1})] transitions of non-bonding electrons present on the nitrogen of the pyrazolines group in Ru(III) complexes. The pattern of the electronic spectra of all the Ru(III) complexes indicates the existence of an octahedral environment around the ruthenium(III) metal ion.[24]

With a view to studying the electrolytic nature of the homoleptic Ru(III) metal complexes **6a–6g**, their molar conductivities were measured in methanol. The molar conductivities (Λ_M) values of the homoleptic Ru(III) complexes are in the range of 174–195 Ω^{-1} cm^2 mol^{-1} at room temperature, indicating electrolytic nature and three counter ion existing outside the coordination sphere of Ru(III) complexes. So, we conclude that all Ru(III) complexes exhibit ionic in nature.

3.2 LC-MS spectrum analysis

The LC-MS spectrum and probable mass fragmentation pattern of complex **6a** are shown in ESI material 6 and 7† respectively. Mass spectrum of the complex **6a** shows molecular ion peak [M^+] at 1176.4 *m*/*z*. The peaks at 818.8 *m*/*z* and 460.4 *m*/*z* are due to pyrazole ligands attached with ruthenium. The peak at 358.3

m/*z* corresponds to pyrazole moiety. The peaks at 253.3 *m*/*z*, 163.3 *m*/*z*, 105.3 *m*/*z* are due to fragmentation of pyrazole ligand.

3.3 Thermogravimetric (TG) studies

Thermogravimetric analysis is the branch of thermal analysis which examines the mass change of a sample as a function of temperature in the scanning mode or as a function of time in the isothermal mode. Not all thermal events bring about a change in the mass of the sample (for example melting, crystallization or glass transition), but there are some very important exceptions which include desorption, absorption, sublimation, vaporization, oxidation, reduction and decomposition. TG is used to characterize the decomposition and thermal stability of materials under a variety of conditions and to examine the kinetics of the physicochemical processes occurring in the sample. The changes in the mass of material are strongly dependent on the experimental conditions employed. Factors such as sample mass, volume and physical form, shape and nature of the sample holder, nature and pressure of the atmosphere in the sample chamber and scanning rate have important influences on the characteristics of the TG curve.

TGA was carried out at a heating rate of 10 °C per minute in the range of 20–800 °C under N_2 atmosphere. The characteristic thermogravimetric gram (mass loss% to temperature in °C) of complex **6a** (ESI material 8†) shows two distinct mass losses. For any complexes, the water molecule are eliminate namely the crystallization one up to 120 °C, while the coordination one in 120–180 °C temperature range, but here no mass losses occur up to 200 °C. So we concluded absence of crystallization and coordinated water molecules in Ru(III) complexes. The mass loss (26.35%) during first step between 200 to 300 °C corresponds to decomposition of three PF_6^- ions from complex **6a**. The second step (66.05%) corresponds to decomposition of three bidentate ligand, in which six coordinate covalent bonds are involved and leaving behind the metal oxide as residue.

3.4 An electron paramagnetic resonance (EPR) studies

The solid state X-band EPR spectrum of complexes **6a–6g** acquired in the polycrystalline state at room temp using 2,2-diphenyl-1-picrylhydrazyl (DPPH) as a standard (g = 2.0027) showed spectrum, exhibiting both parallel and perpendicular g values.

Table 1 EPR spectral data of synthesized complexes

Complexes	$g_{\parallel}$	$g_{\perp}$	$g_{average}$
6a	2.106	1.976	2.019
6b	2.115	1.985	2.028
6c	2.213	1.991	2.065
6d	2.228	2.012	2.084
6e	2.312	2.086	2.161
6f	2.162	1.983	2.042
6g	2.262	2.053	2.122

The low spin d^5 configuration is a good probe of molecular structure and bonding since the observed 'g' values are very sensitive to small changes in structure and to metal ligand covalency. The EPR spectra of all the Ru(III) complexes exhibit a characteristic of an axially symmetric system with $g_{\perp}$ around 1.976–2.053, $g_{\parallel}$ around 2.106–2.312 and g_{avg} = 2.019–2.122 computed from the formula $g_{avg} = (1/3)(2g_{\perp} + g_{\parallel})$ (Table 1). Overall the position of lines and nature of the EPR spectra of the complexes are characteristic of low spin Ru(III) octahedral complexes[25–27] (ESI material 9†).

3.5 IR spectra of Ru(III) complexes

The IR bands for the Ru(III) complexes derived from the pyrazolines ligands are most convenient in attempting to determine the mode of coordination. The IR spectra of the free pyrazolines ligands show a strong band in the regions 1627–1691 cm^{-1}, corresponding to the ketonic group. Coordination of the pyrazoline ligands to the metal through the ketonic oxygen atom is expected to diminish the electron density in the ketonic group frequency. The band due to the ketonic oxygen at around 1594–1630 cm^{-1} shows a decrease in the stretching frequency for the complexes, and being shifted to lower frequencies indicates the coordination of the ketonic oxygen. Bands in the 557–560 cm^{-1} region are ascribed to the formation of Ru–N bonds. Further, the Ru(III) complexes show strong vibrations near 843 cm^{-1}, which are attributable to the PF_6 group. IR spectra of complexes are shown in ESI material 5.†

3.6 Biological screening of synthesized complexes

3.6.1 *In vitro* antibacterial screening. The minimum concentrations of compounds that induced a complete growth inhibition will be recorded as MICs value. A comparative study of *in vitro* antibacterial activity values of the pyrazolines ligands and their complexes indicates that the metal complexes show enhanced activity against two Gram(+ve) and three Gram(−ve) bacteria when incorporated to the pyrazolines ligand. An satisfactory reason for this increase in antibacterial activity may be considered in the light of Overtone's concept[14] and chelation theory.[28] According to Overtone's concept of cell permeability, the lipid membrane that surrounds cell favours the passage of only lipid soluble materials, so that liposolubility is an important factor which controls bacteriostatic activity. On chelation, the polarity of the Ru(III) ion will be lowered to a greater extent due to the overlap of the ligand orbital and partial sharing of the positive charge of the Ru(III) ion with donor groups. Further, it increases the delocalization of π-electrons over whole chelate ring and enhances lipophilicity of the complexes. This increased lipophilicity enhances the penetration of the complexes into lipid membranes and blocks the metal binding sites in bacterial enzymes. The complexes also disturb the respiratory processes of the cell and thus block the synthesis of proteins, which restricts further growth of the organism.

The results concerning MIC values of ligands and their complexes are represented in ESI material 10.† From Fig. 1, we observed that the antibacterial activity of all complexes against five microorganisms better than that of respective ligands. The

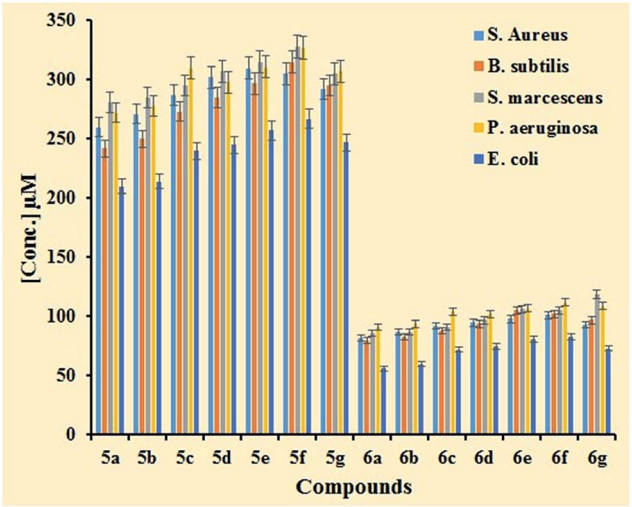

Fig. 1 Effect of different concentration of free ligands and synthesized complexes on Gram(+ve) and Gram(−ve) bacteria. Error bars represent standard deviation of three replicates.

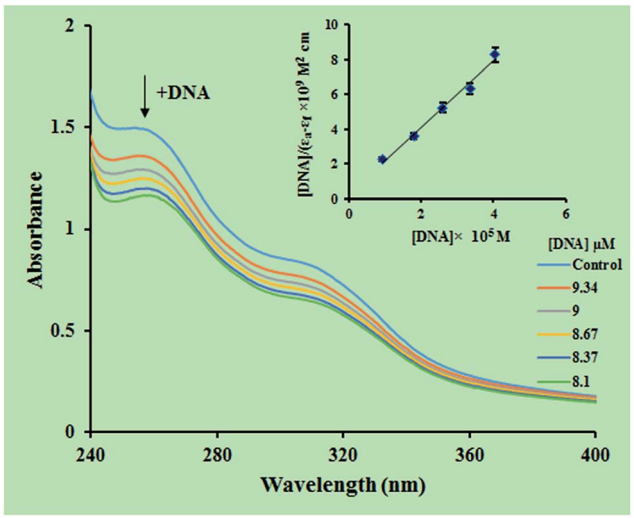

Fig. 2 Absorption spectral changes on addition of HS DNA to the solution of complex **6a** after incubating it for 10 minutes at room temperature in phosphate buffer (Na_2HPO_4/NaH_2PO_4, pH = 7.2). Inset: plot of $[DNA]/(\varepsilon_a - \varepsilon_f)$ *vs.* [DNA]. Error bars represent standard deviation of three replicates (arrow shows the change in absorption with increase in concentration of DNA).

results indicated that a lower concentration of complex **6a** was required to inhibit the bacterial growth and kill the bacterial strain, leading to a higher efficiency in antibacterial activities. Complex **6a** is the most active amongst all the complexes due to presence of fluorine atom at *para* position. Presence of more electronegative environment in complex **6a** improves its biological property. All the complexes show better activity against *S. aureus*, *E. coli* and *P. aeruginosa* than those of $[Ru(phen)_3]^{2+}$, $[Ru(Me_2phen)_3]^{2+}$ and lower than $[Ru(Me_4phen)_3]^{2+}$ reported by Fangfei Li *et al.*[29] and comparable activity against *S. aureus* than those of reported by P.-L. Lam *et al.*[30]

3.6.2 DNA binding study by absorption spectral analysis. Electronic absorption spectroscopy is one of the most useful techniques for DNA-binding studies of metal complexes. The binding ability of the complexes with HS DNA can be characterized by measuring their effects on absorption spectra. Ruthenium metal complexes integrate with DNA have three binding mechanisms namely intercalative-binding model, groove binding model and electrostatic-binding model (binding to the phosphate group).[31] Complexes binding to DNA through intercalation usually result in hypochromism and bathochromism (red shift).[32] When the complex intercalates with base pairs of DNA, the π* orbital of the intercalated ligand of the complex couples with π orbital of the base pairs of DNA, thus decreasing the π–π* transition energy and resulting in the bathochromism.[33] The intrinsic DNA binding constants (K_b) of the complexes to HS DNA were quantitatively determined by observing the change in the absorption intensity of the spectral bands by subsequent addition of HS DNA. An absorption spectrum of complexes with HS DNA was recorded for a constant concentration of complexes (20 µM) with varying concentration of DNA (100 µM) to obtain different DNA/complex mixing ratio is shown in Fig. 2.

The absorption spectral changes were monitored in the intra-ligand charge transfer (ILCT) band around 250–270 nm for the investigation of DNA binding mode and strength. As the DNA concentration is increased, the ILCT transition bands of complexes **6a–6g** exhibit hypochromicity [hypochromicity, $H\% = [(A_{free} - A_{bound})/A_{free}] \times 100\%$] of about 18.47–22.10 ± 0.87%, and bathochromicity of 2–4 nm. The complex **6a** has highest percentage hypochromicity (22.10 ± 0.82%). These spectral characteristics may suggest a mode of binding that involves a stacking interaction between the aromatic chromophore and the DNA base pairs.

In order to elucidate the binding strength of the complexes, the DNA-binding constants K_b were determined by monitoring the changes of absorbance in the ILCT band with increasing concentration of HS DNA. The K_b values of ruthenium complexes were found in the range 2.42 (±0.28) × 10^5 to 6.07 (±0.77) × 10^5 M^{-1} and are higher than that of free ligands (ESI material 11†). It is lower than K_b value of classical intercalators ethidium bromide (7.16 × 10^5 M^{-1}), $[Ru(PEF)Cl_2(H_2O)_2]\cdot 5H_2O$ (5.00 × 10^7 M^{-1})[34] and $[Ru(bpy)_2(dppz)]^{2+}$ (4.90 × 10^6 M^{-1})[35] but higher than $[RuCl(AsPh_3)L^2]$ (3.6 × 10^4 M^{-1}),[36] $[RuCl(AsPh_3)L^3]$ (3.2 × 10^4 M^{-1}),[36] $[Ru(bzimpy)(bpy)(OH_2)]^{2+}$ (3.58 × 10^4 M^{-1}),[37] $[Ru(bzimpy)(phen)(OH_2)]^{2+}$ (2.87 × 10^4 M^{-1})[37] and comparable with $[RuCl(AsPh_3)L^1]$ (4.7 × 10^5 M^{-1}) reported by Govindan Prakash *et al.*[36] From the K_b value and red shift, it is clear that the complexes bind to the DNA by intercalation mode and complex **6a** has the highest binding ability (Fig. 3) than the other complexes due to an existence of fluorine atom. An existence of fluorine atoms act as not only chemical isosteres for the oxygen atoms in the heterocyclic base of thymidine, but also participate in "strong" F–H bonding as a result it shows better antibacterial and DNA interaction activity than other. The binding mode is further confirmed by hydrodynamic volume (*i.e.* viscosity) measurement.

3.6.3 DNA binding study by hydrodynamic volume measurement. To understand the nature of the interaction

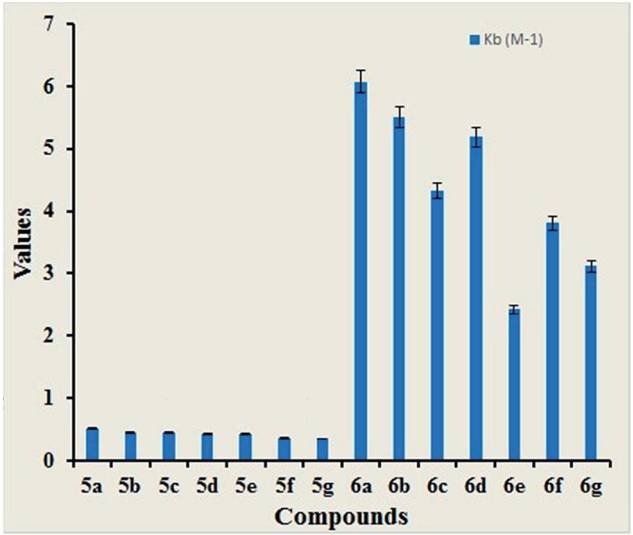

Fig. 3 Plot of K_b values (from absorption titration) of synthesized complexes in M^{-1}. Error bars represent standard deviation of three replicates.

between the complexes and DNA and as a means for further clarifying the binding of the Ru(III) complexes, viscosity measurements of solutions containing HS DNA incubated with the complexes were carried out. In classical intercalation, the DNA helix lengthens as base pairs are separated to accommodate the bound ligand, leading to increase in DNA viscosity, whereas a partial, non-classical ligand intercalation causes a bend in the DNA helix, reducing its effective length and thereby its viscosity. Therefore viscosity measurement is regarded as the least ambiguous and the most critical means for studying the binding mode of metal complexes with DNA in solution and provides stronger arguments for intercalative binding mode.[13]

The effects of Ru(III) complexes on the viscosity of HS DNA are shown in Fig. 4. As illustrated in this figure, on increasing the amount of the Ru(III) complexes the relative viscosity of HS DNA increases steadily, which confirms that the Ru(III) complexes are bound to HS DNA by intercalation. This phenomenon may be explained by the insertion of the compounds between the DNA base pairs, leading to an increase in the separation of base pairs at intercalation sites and thus an increase in overall DNA length. It is clear from the figure that all these complexes show an increase in the relative viscosity of HS DNA. The increase in the degree of viscosity of all compounds depends on their affinity to DNA, with an order as follows: I > II > III > IV > VII > V > VI > ligands (ESI material 12†). This behavior is similar to that of ruthenium complexes reported by Ihtshamul Haq *et al.*,[38] Caipihg. Tan *et al.*[39,40] The viscosity results may reveal the tendency of each ligand to intercalate into DNA base pairs. The increase in DNA viscosity observed in the complexes suggests a classical intercalative mode.

3.6.4 Molecular docking study with HS DNA. Molecular docking study has played important roles in understanding the metal based drug–DNA interactions for rational drug design and discovery, as well as in the mechanistic study by placing a small molecule into the binding site of the target specific area of DNA. Molecular docking studies of the Ru(III) complexes with the DNA duplex of sequence $d(ACCGACGTCGGT)_2$ were performed to predict the chosen binding site along with the preferred orientation of complex inside the DNA helix (Fig. 5). The study shown that the complexes under investigation interact with DNA *via* an intercalation mode involving outside edge stacking interaction with oxygen atom of the phosphate backbone. From the ensuing docked structures, it is clear that the complexes fit well into the intercalative mode of the targeted DNA and A–T rich region stabilized by van der Waal's interaction and hydrophobic contacts.[41,42] The resulting binding energies of docked complexes **6a–g** were found to be −353.38, −375.25, −324.19, −337.93, −355.65, −370.17 and 415.81 kJ mol^{-1}, respectively. The more negative the relative binding values, the more potent is the binding between DNA and target molecules. Thus, we can accomplish that there is a mutual complement between spectroscopic techniques and molecular docked model, which substantiate our spectroscopic results, and provide further evidence of intercalative binding.

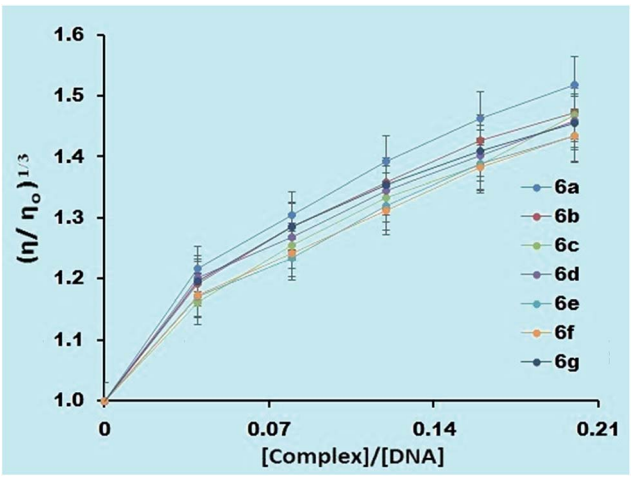

Fig. 4 Effect on relative viscosity of HS DNA under the influence of increasing amounts of complexes at 27 (±0.1) °C in phosphate buffer at pH = 7.2. Error bars represent standard deviation of three replicates.

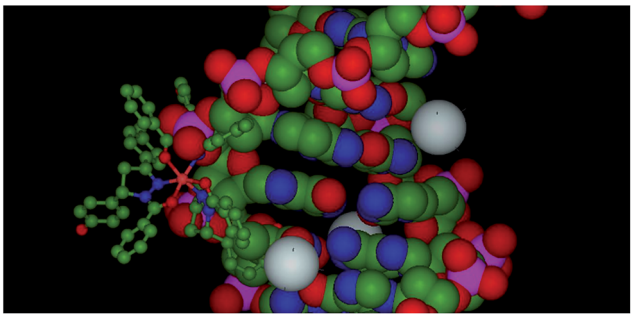

Fig. 5 Molecular docking of the complexes **6a** (ball and stick) with the DNA duplex (VDW spheres) of sequence $d(ACCGACGTCGGT)_2$. The complex is docked in to the DNA showing intercalation between the DNA base pairs.

3.6.5 DNA cleavage screening by chemical nuclease activity. The cleavage reaction on plasmid DNA induced by ruthenium(III) complexes can be monitored by agarose gel electrophoresis. Agarose gel electrophoresis is a convenient method to assess cleavage of DNA by metal complexes to assess the factors affecting the nucleolytic efficiency of a complex and to compare the nucleolytic property of different metal complexes. The DNA cleavage can occur by hydrolytic and oxidative pathways, in which hydrolytic DNA cleavage involves cleavage of phosphodiester bond to generate fragments which can be subsequently relegated; started in a modest way of converting supercoil (SC) form of DNA to the open-circular (OC) form and last in linear (L) form, is now being used for identifying the percentage of cleavage as a function of concentration of nuclease. Oxidative DNA cleavage involves either oxidation of the deoxyribose moiety by abstraction of sugar hydrogen or oxidation of nucleobases.[14]

Fig. 6 illustrates the cleavage of pUC19 DNA induced by the compounds under aerobic conditions. This clearly show that the relative binding efficacy of complexes to DNA is much higher than the binding efficacy of ruthenium salt and free ligands (Fig. 7 and ESI material 14†). The difference in DNA-cleavage efficiency of complexes was due to the difference in binding affinity of complexes to DNA. The similar behavior of Ru(III) complexes with plasmid DNA was shown by reported compounds of type $[Ru(PFL)(PPh_3)_2Cl_2]$,[43] $[Ru(OFL)(PPh_3)_2Cl_2]$,[43] $[Ru(SFL)(PPh_3)_2Cl_2]$,[43] *cis*,*fac*-$[RuCl(dmso\text{-}S)_3(L)]$,[44] *mer*-$[RuCl_3(dmso)(N–N)]$.[40]

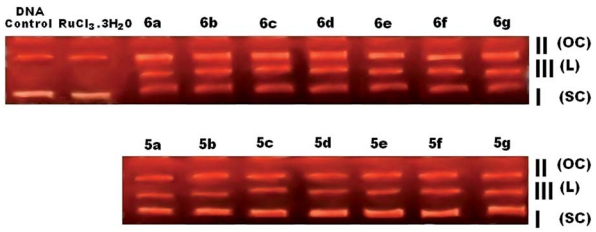

Fig. 6 Photogenic view of cleavage of pUC19 DNA (300 μg cm^{-3}) with series of compounds using 1% agarose gel containing 0.5 μg cm^{-3} EtBr. All reactions were incubated in TE buffer (pH 8) at a final volume of 15 mm^3 for 24 h at 37 °C. Lane 1 DNA control, lane 2 $RuCl_3 \cdot 3H_2O$, lane 3 **6a**, lane 4 **6b**, lane 5 **6c**, lane 6 **6d**, lane 7 **6e**, lane 8 **6f**, lane 9 **6g**, lane 10 **5a**, lane 11 **5b**, lane 12 **5c**, lane 13 **5d**, lane 14 **5e**, lane 15 **5f** and lane 16 **5g**.

The principle of this method is that molecules migrate in the gel as a function of their mass, charge and shape, with super-coiled DNA migrating faster than open circular molecules of the same mass and charge. The native DNA remains in the super-coiled (SC) form, also known as covalently coiled coil DNA, here designated as Form I. Single strand cleavage results in so called nicked or open circular (OC) form of DNA (designated as Form II), whereas the double-strand cleavage results in linear (LC) form of DNA (designated as Form III). The migration rate during agarose gel electrophoresis depends on both size (base pairs) and conformation, with smaller or condensed DNA migrating faster than larger or unfolded DNA. Form I has a tightly packed conformation and therefore migrates faster through agarose gels than linear DNA (intermediate migration) or open circle DNA (slowest migration).

3.6.6 *In vitro* cytotoxic study. All the synthesized compounds were screened for their cytotoxicity (brine shrimp bioassay) using the protocol of Meyer *et al.*[18] The shrimp lethality assay is considered as a useful tool for preliminary assessment of toxicity. Brine shrimp lethality bioassay is a development in the assay procedure of bioactive compound, which indicates cytotoxicity as well as a wide range of pharmacological activities of the compounds. The method is inexpensive, rapid, reliable and economical.

Results for the lethality were noted in terms of deaths of larvae. The mortality rate of brine shrimp nauplii was found to increase with increasing the concentration of complexes. A plot of the log of sample's concentration *versus* percentage of mortality showed a linear correlation. From the graph, the LC_{50}

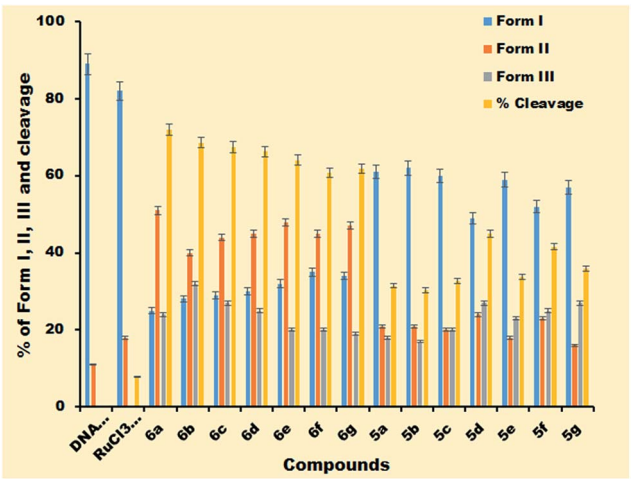

Fig. 7 Plot of DNA cleavage data by agarose gel electrophoresis of different compounds. Error bars represent standard deviation of three replicates.

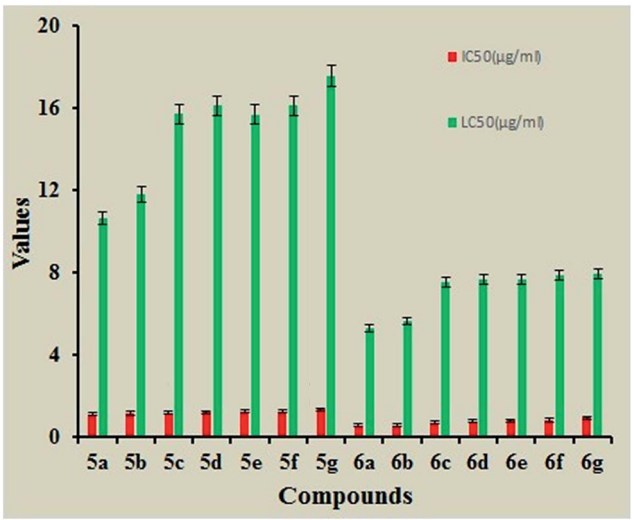

Fig. 8 Plot of LC_{50} values and IC_{50} values of different compounds in μg mL^{-1}. Error bars represent standard deviation of three replicates.

values of the compounds were calculated, and they were found in the range of 5.296 to 17.579 μg mL^{-1} (ESI material 11†). From the data recorded, complex **6a** is the most potent amongst all the compounds. From Fig. 8, it is concluded that the synthesized complexes are good cytotoxic agent than that of respective ligands. The order of potency of compounds is **6a** > **6b** > **6c** > **6d** > **6g** > **6e** > **6f**. The degree of lethality was found to be directly proportional to the concentration of the compounds. The mortality rate of brine shrimp nauplii was found to increase with increasing the concentration of complexes. The tested Ru(III) complexes have strong cytotoxic activity but this examination is a primary one and further tests are required to investigate its actual mechanism of cytotoxicity and its probable effects on higher animal model and on cancer cell line. It recommends that the complexes can be used as potent cytotoxic agents with the hope of adding arsenal of weapons used against the fatal disease cancer.

3.6.7 Cellular level bioassay. In the present study, *S. pombe* cells has been used to study cytotoxic effect of compounds at a cellular level. *S. pombe* cells has become an important tool to study cell biology due to its eukaryotic and fairly big size characteristics. A comparative study of cellular level cytotoxicity values of the free ligands and their complexes indicates that the metal complexes show better activity against *S. pombe* cells compared to the pyrazolines ligand. Cell death caused by toxicity of the chemically synthesized compounds could be easily monitored by vital staining (Fig. 9). The toxicity was found to vary with the type of substituent present and concentrations of the synthesized compounds. General observation is that as concentration of compounds increased the cytotoxicity was also increased. After 17 hours of the treatment, many of the *S. pombe* cells were killed due to toxic nature of the compound. The results concerning % viability of free ligands and their complexes are represented in ESI material 15.† From Fig. 10, we observed that the cytotoxicity activity of all complexes against *S. pombe* cells better than that of respective free ligands. Complex **6a** is the most active amongst all the compounds.

3.6.8 *In vitro* antimalarial study. As part of this search for novel drugs against malaria, we report encouraging results for seven new compounds resulting from the modification of pyrazolines moiety by coordination to ruthenium metal centres; the new complexes are highly active against a chloroquine resistant strain of *Plasmodium falciparum*. Malaria is one of the most prevalent infectious diseases worldwide and it represents a major global health issue for which new effective chemotherapies are urgently needed.

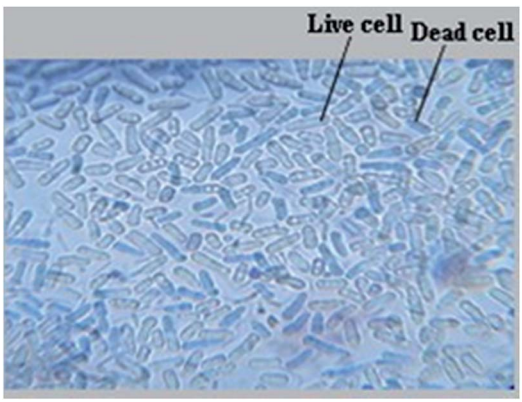

Fig. 9 Effect of compounds on *S. pombe* cells. Dead cells are seen dark whereas live cells are seen transparent.

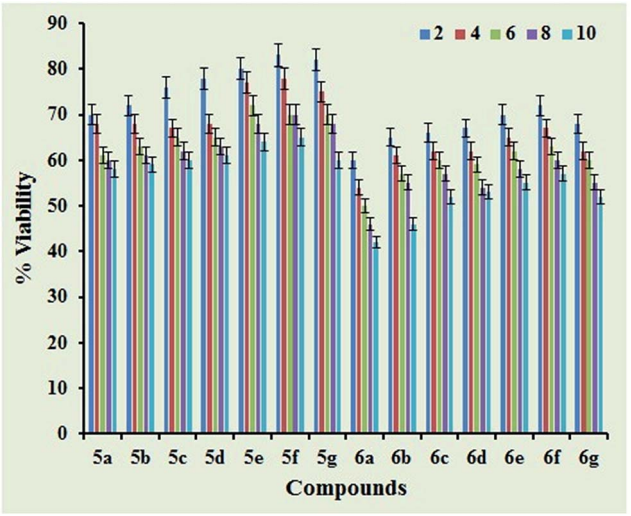

Fig. 10 Effect of compounds on viability of *S. Pombe* cells at different concentrations. Error bars represent standard deviation of three replicates.

All newly synthesized complexes were evaluated for their *in vitro* antimalarial activity, which clearly shows the advantage of ruthenium complexation and the requirement of six coordinated geometry around ruthenium as some of the key structural features for designing such metal-based antimalarial agent. The results of the pharmacological screening are expressed as the drug concentration resulting in 50% inhibition (IC_{50}) of parasite growth. The mean values of IC_{50} in μg mL^{-1} for all complexes and respective ligands are given in ESI material 11.† Fig. 8 shows that all complexes exhibit good antimalarial activity than respective ligands (0.54–1.34 μg mL^{-1}). It is thus clear that the combination of ruthenium metal and pyrazolines ligand in a single molecule does produce an enhancement of the activity against resistant strains of the parasite, demonstrating the validity of our concept in the search for novel antimalarial drugs capable of overcoming resistance. The IC_{50} values of all Ru(III) complexes are comparable to $[Ru(A)_2(B)]Cl_2$ (10 μg mL^{-1}),[45] [Cu(terpyridyl)Cl]Cl (0.52 μM), $Fe(terpyridyl)Cl_3$ (0.63 μM).[46]

4. Conclusions

The objective of the present article is to synthesize, characterize and examine the biological activities of some newly functionalized pyrazolines based homoleptic Ru(III) compounds in search of new drugs looking promising as potent antimalarial, antimicrobial, DNA binding, DNA cleavage and cellular level cytotoxic agents. This synthetic approach allows the incorporation of potent bioactive nuclei in a single skeleton through an

easy way and were carried out with an aim to study their biological activity. Data of magnetic behavior, electronic spectral and ESR measurement points towards the d^5 system with an octahedral environment around the metal ion. The molar conductivities values of synthesized metal complexes are indicates, three counter ion present outside the coordination sphere which accomplish all Ru(III) complexes are ionic in nature. The antimicrobial activity of the complexes has been tested on different microorganisms and the data show an enhanced biological activity in relation to the free ligands. Hypochromism and bathochromism of band in absorption titration and increase in relative viscosity of DNA recommend that all complexes bind with DNA *via* classical intercalative mode. Complex **6a** is bound more strongly than the other complexes due to presence of fluorine atom at 4^{th} position of aromatic ring. Presence of fluorine atoms act as not only chemical isosteres for the oxygen atoms in the heterocyclic base of thymidine, but also participate in "strong" F–H bonding as a result it shows superior antibacterial and DNA interaction activity than other. Molecular docking studies of the complexes with the DNA duplex of sequence $d(ACCGACGTCGGT)_2$ were performed to predict the chosen binding site which suggests intercalation between complex and DNA base pairs. The DNA cleavage study of pUC19 shows that all complexes have high cleavage ability than metal salt and ligands. All the complexes show strong *in vitro* cytotoxic, *in vitro* antimalarial as well as cellular level bioassay. Presence of more electronegative environment in complex **6a** improves its biological property. The preliminary studies encourage for carrying out further *in vivo* experiments.

Conflict of interest

The authors report no conflicts of interest. The authors alone are responsible for the content and writing of the paper.

Acknowledgements

The authors thankful to the Head, Department of Chemistry, Sardar Patel University, Vallabh Vidyanagar, Gujarat, India, for providing the laboratory facilities, Dhanji P. Rajani, microcare laboratory, Surat for *in vitro* antimalarial activity, IIT SAIF, Bombay for EPR analysis, DST-PURSE, Sardar Patel University, Vallabh Vidyanagar for LC-MS analysis, U.G.C., New Delhi for providing financial assistance of UGC BSR grant No. C/2013/BSR/Chemistry/59, UGC CAS and "UGC BSR One Time Grant", vide UGC letter No. F.19-119/2014(BSR).

Notes and references

1 K. E. Erkkila, D. T. Odom and J. K. Barton, *Chem. Rev.*, 1999, **99**, 2777–2796.
2 C. Metcalfe and J. A. Thomas, *Chem. Soc. Rev.*, 2003, **32**, 215–224.
3 D. S. Johnson and D. L. Boger, *Comprehensive Supramolecular Chemistry*, Pergamon, Oxford, 1996.
4 A. Sigel and H. Sigel, Metal Ions and Their Complexes in Medication, in *Metal Ions in Biological Systems*, New York, 2004.
5 A. Sigel and H. Sigel, Metal Complexes in Tumor Diagnosis and As Anticancer Agents, in *Metal Ions in Biological Systems*, 2004.
6 S. Fletcher, E. P. Keaney, C. G. Cummings, M. A. Blaskovich, M. A. Hast, M. P. Glenn, S.-Y. Chang, C. J. Bucher, R. J. Floyd, W. P. Katt, M. H. Gelb, W. C. van Voorhis, L. S. Beese, S. M. Sebti and A. D. Hamilton, *J. Med. Chem.*, 2010, **53**, 6867–6888.
7 A. Tanitame, Y. Oyamada, K. Ofuji, M. Fujimoto, N. Iwai, Y. Hiyama, K. Suzuki, H. Ito, H. Terauchi, M. Kawasaki, K. Nagai, M. Wachi and J.-I. Yamagishi, *J. Med. Chem.*, 2004, **47**, 3693–3696.
8 G. Ouyang, X.-J. Cai, Z. Chen, B.-A. Song, P. S. Bhadury, S. Yang, L.-H. Jin, W. Xue, D.-Y. Hu and S. Zeng, *J. Agric. Food Chem.*, 2008, **56**, 10160–10167.
9 A. Hall, A. Billinton, S. H. Brown, N. M. Clayton, A. Chowdhury, G. M. P. Giblin, P. Goldsmith, T. G. Hayhow, D. N. Hurst, I. R. Kilford, A. Naylor, B. Passingham and L. Winyard, *Bioorg. Med. Chem. Lett.*, 2008, **18**, 3392–3399.
10 B. P. Bandgar, S. S. Gawande, R. G. Bodade, N. M. Gawande and C. N. Khobragade, *Bioorg. Med. Chem.*, 2009, **17**, 8168–8173.
11 S. C. Karad, V. B. Purohit, D. K. Raval, P. N. Kalaria, J. R. Avalani, P. Thakor and V. R. Thakkar, *RSC Adv.*, 2015, **5**, 16000–16009.
12 D. Sinha, A. K. Tiwari, S. Singh, G. Shukla, P. Mishra, H. Chandra and A. K. Mishra, *Eur. J. Med. Chem.*, 2008, **43**, 160–165.
13 J. V. Mehta, S. B. Gajera, D. D. Patel and M. N. Patel, *Appl. Organomet. Chem.*, 2015, **29**, 357–367.
14 J. V. Mehta, S. B. Gajera and M. N. Patel, *Spectrochim. Acta, Part A*, 2015, **136**, 1881–1892.
15 W. Zhong, J.-S. Yu and Y. Liang, *Spectrochim. Acta, Part A*, 2003, **59**, 1281–1288.
16 M.-L. Liu, M. Jiang, K. Zheng, Y.-T. Li, Z.-Y. Wu and C.-W. Yan, *J. Coord. Chem.*, 2014, **67**, 630–648.
17 J. Yang, R. N. S. Wong and M. S. Yang, *Chem.-Biol. Interact.*, 2000, **125**, 221–232.
18 B. N. Meyer, N. R. Ferrigni, J. E. Putnam, L. B. Jacobsen, D. E. Nichols and J. L. McLaughlin, *Planta Med.*, 1982, **45**, 31–34.
19 M. R. Islam, S. M. R. Islam, A. S. M. Noman, J. A. Khanam, S. M. M. Ali, S. Alam and M. W. Lee, *Mycobiology*, 2007, **35**, 25–29.
20 W. Trager and J. Jensen, *Science*, 1976, **193**, 673–675.
21 M. M. T. Khan, D. Srinivas, R. I. Kureshy and N. H. Khan, *Polyhedron*, 1991, **10**, 2559–2565.
22 C. J. Ballhausen, *Introduction to Ligand Field Theory*, McGarw Hill, New York, 1962.
23 A. B. P. Lever, *Inorganic Electronic Spectroscopy*, Elsevier, New York, 2nd edn, 1984.

24 R. Samanta, B. Mondal, P. Munshi and G. Kumar Lahiri, *J. Chem. Soc., Dalton Trans.*, 2001, 1827–1833, DOI: 10.1039/B100163I.
25 M. M. T. Khan, D. Srinivas, R. I. Kureshy and N. H. Khan, *Inorg. Chem.*, 1990, **29**, 2320–2326.
26 R. Ramesh and S. Maheswaran, *J. Inorg. Biochem.*, 2003, **96**, 457–462.
27 O. K. Medhi and U. Agarwala, *Inorg. Chem.*, 1980, **19**, 1381–1384.
28 B. G. Tweedy, *Phytopathology*, 1964, **55**, 910.
29 F. Li, Y. Mulyana, M. Feterl, J. M. Warner, J. G. Collins and F. R. Keene, *Dalton Trans.*, 2011, **40**, 5032–5038.
30 P. L. Lam, G. L. Lu, K. M. Hon, K. W. Lee, C. L. Ho, X. Wang, J. C. O. Tang, K. H. Lam, R. S. M. Wong, S. H. L. Kok, Z. X. Bian, H. Li, K. K. H. Lee, R. Gambari, C. H. Chui and W. Y. Wong, *Dalton Trans.*, 2014, **43**, 3949–3957.
31 C. V. Kumar and E. H. Asuncion, *J. Am. Chem. Soc.*, 1993, **115**, 8547–8553.
32 J. R. J. Sorenson, *J. Med. Chem.*, 1984, **27**, 1747–1749.
33 R. Indumathy, S. Radhika, M. Kanthimathi, T. Weyhermuller and B. Unni Nair, *J. Inorg. Biochem.*, 2007, **101**, 434–443.
34 H. Muslu, A. Golcu, M. Tumer and M. Ozsoz, *J. Coord. Chem.*, 2011, **64**, 3393–3407.
35 Y.-J. Liu, Z.-H. Liang, Z.-Z. Li, C.-H. Zeng, J.-H. Yao, H.-L. Huang and F.-H. Wu, *BioMetals*, 2010, **23**, 739–752.
36 G. Prakash, R. Manikandan, P. Viswanathamurthi, K. Velmurugan and R. Nandhakumar, *J. Photochem. Photobiol., B*, 2014, **138**, 63–74.
37 V. G. Vaidyanathan and B. U. Nair, *Dalton Trans.*, 2005, 2842–2848, DOI: 10.1039/b502917a.
38 I. Haq, P. Lincoln, D. Suh, B. Norden, B. Z. Chowdhry and J. B. Chaires, *J. Am. Chem. Soc.*, 1995, **117**, 4788–4796.
39 C. Tan, J. Liu, H. Li, W. Zheng, S. Shi, L. Chen and L. Ji, *J. Inorg. Biochem.*, 2008, **102**, 347–358.
40 C. Tan, J. Liu, L. Chen, S. Shi and L. Ji, *J. Inorg. Biochem.*, 2008, **102**, 1644–1653.
41 E. F. Pettersen, T. D. Goddard, C. C. Huang, G. S. Couch, D. M. Greenblatt, E. C. Meng and T. E. Ferrin, *J. Comput. Chem.*, 2004, **25**, 1605–1612.
42 S. Tabassum, M. Zaki, M. Afzal and F. Arjmand, *Dalton Trans.*, 2013, **42**, 10029–10041.
43 M. Patel, H. Joshi and C. Patel, *J. Chem. Sci.*, 2014, **126**, 739–749.
44 R. Gaur, R. A. Khan, S. Tabassum, P. Shah, M. I. Siddiqi and L. Mishra, *J. Photochem. Photobiol., A*, 2011, **220**, 145–152.
45 S. S. Anchuri, S. Thota, R. N. Bongoni, R. Yerra, R. N. Reddy and S. Dhulipala, *J. Chin. Chem. Soc.*, 2013, **60**, 153–159.
46 J. Paraskevopoulosa, P. Smithc, H. Hopped, D. Choprae, T. Govenderb, H. Krugera and G. Maguirea, *S. Afr. J. Chem.*, 2013, **66**, 80–85.

